

Energy & Environmental Science

Accepted Manuscript



This is an *Accepted Manuscript*, which has been through the Royal Society of Chemistry peer review process and has been accepted for publication.

Accepted Manuscripts are published online shortly after acceptance, before technical editing, formatting and proof reading. Using this free service, authors can make their results available to the community, in citable form, before we publish the edited article. We will replace this *Accepted Manuscript* with the edited and formatted *Advance Article* as soon as it is available.

You can find more information about *Accepted Manuscripts* in the [Information for Authors](#).

Please note that technical editing may introduce minor changes to the text and/or graphics, which may alter content. The journal's standard [Terms & Conditions](#) and the [Ethical guidelines](#) still apply. In no event shall the Royal Society of Chemistry be held responsible for any errors or omissions in this *Accepted Manuscript* or any consequences arising from the use of any information it contains.

Broader context

The electrolysis of water to hydrogen is recognized as a front-running technology for the energy storage and conversion from the renewable sources such as the solar and wind power. One of the key reactions for this technology, i.e. hydrogen evolution reaction (HER) is currently high-cost due to the massive use of the precious Pt-based catalysts. It is urgent to employ low-cost and earth-abundant materials to replace the precious-metal catalysts in order to make this technology become more economical. However, most non-precious metals, especially the very abundant 3d transition metals are not stable in acidic medium, usually leading a severely degraded activity. Herein, we demonstrated a strategy for the non-precious-metal catalysts with high activity and long-term durability towards HER via encapsulating Fe, Co and FeCo alloy into N-doped carbon nanotubes (NCNTs). In this system, these 3d metals are protected by the carbon wall around them, and thereby do not directly contact with the acidic electrolyte, while the exotic activity for HER originates from the electron transfer from the metals, which further modify the electronic structure of the carbon surface. This work paves a new route in the design of efficient and durable non-precious-metal electrocatalysts for HER in acidic medium.

Highly active and durable non-precious-metal catalyst encapsulated in carbon nanotubes for hydrogen evolution reaction

Jiao Deng,[§] Pengju Ren,[§] Dehui Deng,* Liang Yu, Fan Yang, Xinhe Bao*

State Key Laboratory of Catalysis, Dalian Institute of Chemical Physics, Chinese Academy of Sciences, Zhongshan Road 457, Dalian 116023, China.

[§]These authors have contributed equally.

*E-mail: dhdeng@dicp.ac.cn; xhbao@dicp.ac.cn; Fax: +86-411-84379128; Tel: +86-411-84686637.

Abstract

Employing a low-cost and highly efficient electrocatalyst to replace Pt-based catalysts for hydrogen evolution reaction (HER) has attracted increasing interest in renewable energy research. Earth-abundant transition metals such as Fe, Co and Ni have been investigated as promising alternatives in alkaline electrolytes. However, these non-precious-metal catalysts are not stable in acids, excluding their application in the acidic solid polymer electrolyte (SPE). Herein, we report a strategy to encapsulate 3d transition metals Fe, Co and the FeCo alloy into nitrogen-doped carbon nanotubes (CNTs) and investigated their HER activity in acidic electrolyte. The optimized catalysts exhibited long-term durability and high activity with only a ~70 mV onset overpotential vs. RHE which is quite close to that of commercial 40% Pt/C catalyst, demonstrating the potential for the replacement of Pt-based catalysts. Density function theory (DFT) calculations indicated that the introduction of metal and nitrogen dopants can synergistically optimize the electronic structure of the CNTs and the adsorption free energy of H atom on CNTs, and therefore promote the HER with a Volmer-Heyrovsky mechanism.

Context

The production of H₂ is essential to a few key technologies related to our energy future,¹ for instance the hydrogen fuel cells and the synthesis of liquid fuels from syngas and CO₂. Among current technologies for H₂ production, the electrocatalytic

hydrogen evolution reaction (HER) from water is a process that has attracted much attention due to its high energy conversion efficiency.² So far, Pt-based catalysts are generally considered as the most effective HER electrocatalysts^{3,4} while their commercialization was largely hindered by the high cost and limited supply of Pt. Many research efforts have been devoted to the search of non-precious-metal based HER catalysts in the past decades. Particularly, earth-abundant 3d transition metals (TMs) such as Fe, Co, Ni have been demonstrated as promising catalytic materials for HER in alkaline electrolytes.⁵⁻¹⁰ However, 3d TMs are not stable in acids and therefore exclude their application in acidic solid polymer electrolyte (SPE), which is considered to be more efficient and exquisite for HER compared with the alkaline electrolyser.¹¹ In recent years, molybdenum-based materials, such as MoS₂,¹²⁻¹⁹ MoSe₂,^{14,20} Mo₂C,^{21,22} MoB,²² MoS₂ analogues,²³ NiMoN_x,²⁴ Co_{0.6}Mo_{1.4}N₂,²⁵ have evolved as possible alternatives for HER in acidic electrolytes, while the durability of Mo-based catalysts is still not satisfactory when suffer strongly acidic electrolytes under the long-time operation or accelerated degradation measurements.

Recently, we demonstrated that encapsulated non-precious metals in carbon nanotubes (CNTs) can activate O₂ on the outer carbon surface while the encapsulated metal nanoparticles are protected by the carbon layer from being leached in the acidic medium.^{26,27} Inspired by this, we now designed robust and highly efficient HER electrocatalysts by using N-doped carbon nanotubes (NCNTs) encapsulating 3d TM Fe, Co and FeCo alloy nanoparticles (NPs) via a chemical vapor deposition (CVD) method. These catalysts exhibited high activity and long-term durability towards HER in acidic electrolytes. In combination with DFT calculations, we further investigated the nature of active sites and the mechanism of HER process in this system.

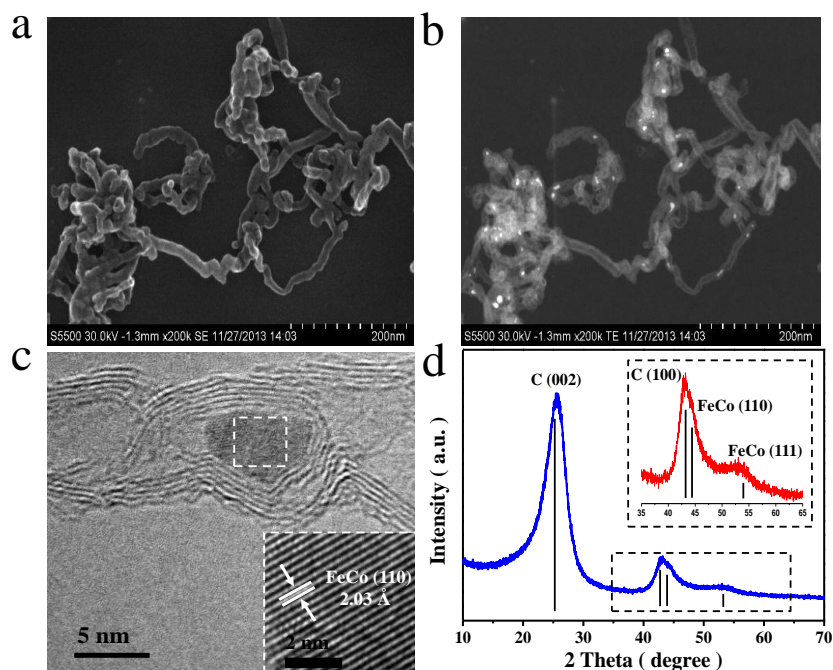


Figure 1. (a) SEM image of FeCo@NCNTs. (b) STEM image of FeCo@NCNTs at the same region with the SEM. (c) HRTEM image of FeCo@NCNTs with the inset showing the (110) crystal plane of the FeCo nanoparticle. (d) XRD pattern of FeCo@NCNTs with the inset showing the partial enlarged detail between the 35 degree and 65 degree.

3d TM Fe, Co and FeCo alloy NPs were encapsulated within the NCNTs through a CVD method. Briefly, pyridine, as the carbon and nitrogen source, was bubbled via Ar onto 3d TM metal NPs supported on MgO, which serve as the catalysts to form NCNTs encapsulating metal NPs at 700 °C. Subsequently, acid treatment was used to remove the MgO support and metals exposed outside NCNTs (see Experimental Section in Supporting Information for more details). The corresponding samples using supported Fe, Co or FeCo alloy NPs as the catalysts were denoted as Fe@NCNTs, Co@NCNTs and FeCo@NCNTs, respectively. Scanning electron microscopy (SEM) image (Figure 1a) shows the tubular morphology of FeCo@NCNTs, and the scanning transmission electron microscopy (STEM) image of the corresponding region shows that metal NPs of c.a. 5-10 nm in diameter have been encapsulated in CNTs (Figure 1b), which was further confirmed by the transmission electron microscopy (TEM) images (Figure S1a and S1b). High resolution (HR) TEM image (Figure 1c) shows

that the metal NPs were completely coated by the graphitic carbon shells with a layer distance of 3.4 Å and no NPs were observed outside the NCNTs. These NPs exhibit a d spacing of 2.03 Å, corresponding to the (110) plane of FeCo alloy. Elemental mapping image of metal NPs by energy dispersive X-ray spectroscopy (EDX) showed that the distribution of Fe and Co in NPs is homogeneous (Figure S1d), consistent with the characterization of X-ray diffraction (XRD) (Figure 1d) showing the structural pattern of FeCo alloys. The metallic character of these NPs provides another evidence that the FeCo NPs were completely encapsulated inside the NCNTs, preventing the oxidation of metal when exposed to air. Likewise, the encapsulation of metallic Fe or Co NPs were also confirmed for Fe@NCNTs and Co@NCNTs catalysts (Figure S2 and S3).

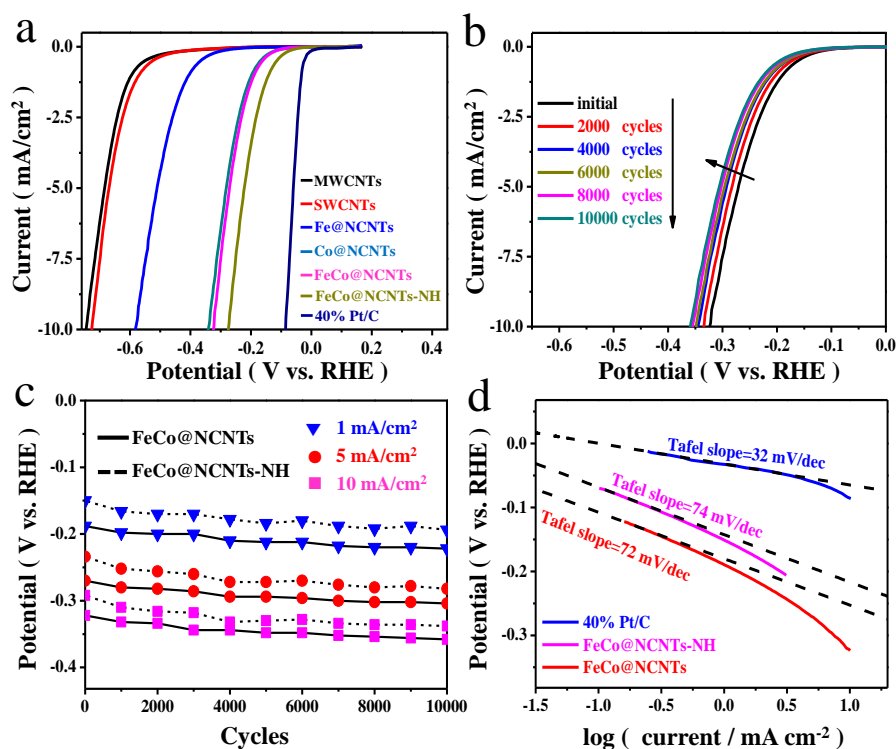


Figure 2. (a) Polarization curves of Fe@NCNTs, Co@NCNTs, FeCo@NCNTs, FeCo@NCNTs-NH along with MWCNTs, SWCNTs and 40% Pt/C for comparison. (b) Durability measurement of FeCo@NCNTs: polarization curves recorded initially and after every 2000 CV sweeps between +0.77 and -0.18 V (vs. RHE) at 100 mV s⁻¹. All the polarization curves were performed in 0.1 M H₂SO₄ at a scan rate of 2 mV s⁻¹. (c) Potential values recorded initially and after every 1000 CV sweeps from the

polarization curves of durability measurements for FeCo@NCNTs and FeCo@NCNTs-NH at 1 mA cm⁻², 5 mA cm⁻², 10 mA cm⁻², respectively. (d) Tafel plots for FeCo@NCNTs, FeCo@NCNTs-NH and 40% Pt/C, respectively.

The typical three-electrode setup was adopted to assess the electrocatalytic HER activities of these NCNTs encapsulating metal catalysts in 0.1 M H₂SO₄. As a reference, we also carried out the measurements of CNTs and commercial 40% Pt/C electrocatalysts. The polarization curves showed that all these catalysts exhibited much higher HER activities than pristine CNTs including both single-wall CNTs (SWCNTs) and multiple-wall CNTs (MWCNTs) as well as N-doped MWCNTs (MWCNTs-NH) in figure 2a and S6a. The HER catalytic activity of Fe@NCNTs, Co@NCNTs and FeCo@NCNTs increased sequentially, and the polarization curve of FeCo@NCNTs showed an onset overpotential of ~110 mV vs. RHE, beyond which the cathodic current rose rapidly under more negative potentials.

Previous studies indicated that nitrogen in metal/carbon composites could significantly promote catalytic reactions, e.g. the oxygen reduction reaction.²⁶⁻³⁰ To study the role of doped nitrogen atoms for HER, we introduced NH₃ during the preparation of electrocatalysts to increase the concentration of nitrogen. These corresponding catalysts are denoted as Fe@NCNTs-NH, Co@NCNTs-NH, FeCo@NCNTs-NH, respectively (see Experimental Section in Supporting Information for more details). Note that, from electron microscopies, these electrocatalysts appear similar as these above electrocatalysts prepared without NH₃. Chemical compositions analysis (Table S1) showed that the nitrogen concentration in Fe@NCNTs-NH, Co@NCNTs-NH and FeCo@NCNTs-NH have all increased compared with the corresponding samples prepared without NH₃. Figure S6a indicates the increase of N concentration in these serial catalysts can enhance the HER activity distinctively compared with the corresponding samples without NH₃ treatment. Remarkably, FeCo@NCNTs-NH showed a very high HER activity with an onset overpotential of only ~70 mV vs. RHE (Figure 2a), which is amongst the

smallest overpotential for non-precious-metal HER catalysts in acidic electrolyte reported so far (see the statistical results in Table S2). These results indicate that the introduction of nitrogen in CNTs-encapsulated metal catalysts can significantly enhance their HER activity.

Durability is another critical measurement in the evaluation of non-precious-metal HER electrocatalysts. In this study, accelerated degradation measurements were adopted to evaluate the durability. The polarization curve was recorded after every 2000 cyclic voltammetric (CV) sweeps between +0.77 and -0.18 V (vs. RHE). As in Figure 2b, the polarization curve of FeCo@NCNTs after 10000 cycles retained almost similar performance to the initial test. The same trend could be observed for FeCo@NCNTs-NH (Figure S6b). Moreover, from the potential values recorded at the same current density of 1 mA cm^{-2} , 5 mA cm^{-2} , 10 mA cm^{-2} before and after test, both FeCo@NCNTs and FeCo@NCNTs-NH exhibited high durability with only a slight increase at the overpotential (Figure 2c). To our knowledge, the long-term durability demonstrated in our measurements is rarely seen or reported for non-precious-metal HER catalysts in acidic media. The high activity combined with remarkable durability of these catalysts illustrates the potential of CNTs-encapsulated non-precious metal catalysts for HER.

To understand the reaction mechanism of HER occurred on CNTs-encapsulated metal catalysts, Tafel slopes, determined for the rate-limiting step of HER, were used to interpret possible elementary steps involved.^{31,32} The Tafel slopes for these catalysts are c.a. 70-120 mV/decade (Figure 2d and S7), e.g. 78 mV/decade for Co@NCNTs (Figure S7) and 72 mV/decade for FeCo@NCNTs (Figure 2d), in the range reported by previous studies on non-precious-metal HER catalysts.^{12-15,20-22,33-40} These Tafel slope values suggest that HER on CNTs-encapsulated metal catalysts would likely occur via a Volmer-Heyrovsky mechanism.^{22,24,41}

Density function theory (DFT) calculations were carried out to understand the origin of the HER activity of these CNTs-encapsulated metal catalysts. It has been demonstrated that the adsorption free energy of H ($\Delta G(\text{H}^*)$) is a good descriptor of

HER on a broad range of catalytic materials.¹² The relation between $\Delta G(\text{H}^*)$ and measured currents presents a volcano curve, meaning a catalyst with moderate adsorption free energy ($\Delta G(\text{H}^*) \approx 0$) could be a good candidate for HER.⁴² The $\Delta G(\text{H}^*)$ on the carbon surface of pristine CNTs encapsulating an Fe_4 cluster (Fe@CNTs) and N-doped CNTs encapsulating an Fe_4 cluster (Fe@NCNTs) are presented in Table 1. Though the sizes of metal particles adopted in the calculations are smaller than that observed experimentally (Figure S8), the essential effect can still be captured by the simple geometry adopted here.²⁶ After the introduction of the enclosed Fe_4 cluster, the $\Delta G(\text{H}^*)$ on carbon decreases remarkably from 1.29 eV to 0.30 eV. Meanwhile, we also calculated the $\Delta G(\text{H}^*)$ on the outer surfaces of CNTs encapsulating a Co_4 cluster (Co@CNTs) and Fe_2Co_2 cluster (FeCo@CNTs) (Table S3), i.e. 0.18 eV and 0.11 eV, respectively, which are even lower compared with that on Fe@CNTs, implying the introduction of Co is more efficient for HER, consistent with the experimental results. Upon introducing N atom into the carbon lattice of Fe@CNTs, the $\Delta G(\text{H}^*)$ further decreases to -0.05 eV. Therefore, the nitrogen doping and enclosed metal cluster can significantly promote the hydrogen adsorption on CNTs synergistically.

Table 1. Adsorption free energy of H ($\Delta G(\text{H}^*)$) (in eV) for various models.

Structure	$\Delta G(\text{H}^*)$
Pure CNTs	1.29
NCNTs	0.42
Fe@CNTs	0.30
Fe@NCNTs	-0.05

The interaction between adsorbed H and carbon sites of Fe@CNTs is mainly covalent. The adsorption of H atom on pristine CNTs is thermodynamically unfavored owing to the inertness of CNT walls. Our previous study showed that the electronic structure near the Fermi level of CNTs can be significantly modified by the iron cluster due to the charge transfer from iron to carbon atoms nearby.²⁶ In this study, the

band center of the occupied states of C-H bond (sum of C_{2p} and H_{1s}) on Fe@CNTs are located in a lower energy regime than that on pristine CNTs (Figure 3a), indicating that a stronger H-C chemical bonding can be formed on carbon surface of Fe@CNTs. The electronic state structure analysis reveals that the stabilization of H^* species in HER process may originate from the enriched charge density of carbon atoms near iron cluster (Figure S9) as well as nitrogen dopants.

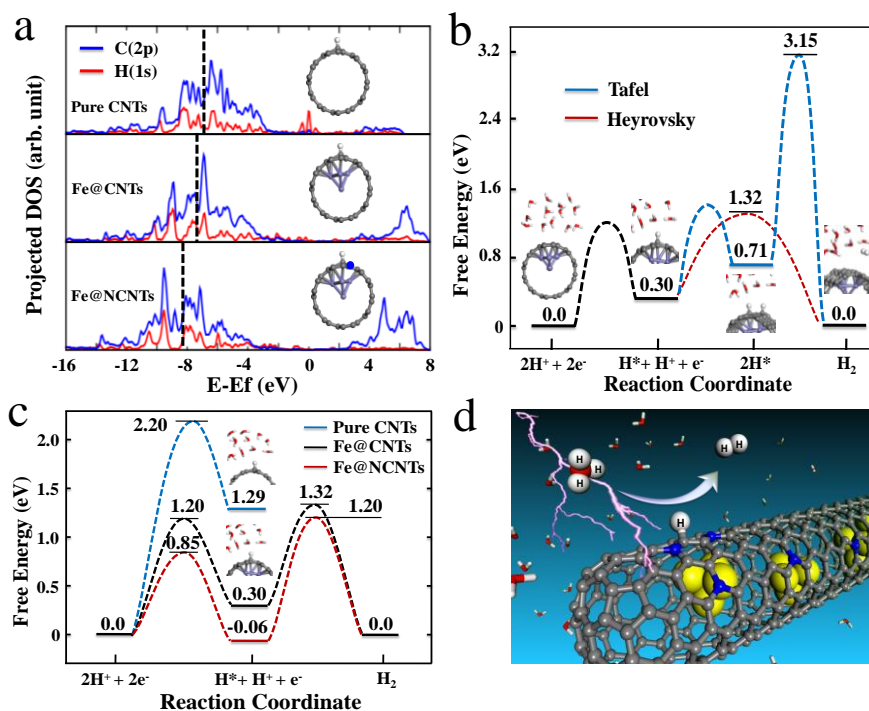
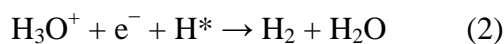


Figure 3. (a) Comparison of projected density of states (DOS) of H(1s) and its bonded C(2p) when H is adsorbed on the surface of pristine CNTs, Fe@CNTs, and Fe@NCNTs. The dashed lines present the center of the occupied band. (b) The free energy profiles of Tafel and Heyrovsky route for Fe@CNTs. (c) The free energy profiles of Heyrovsky route for pristine CNTs, Fe@CNTs and Fe@NCNTs. (d) A schematic representation of the HER process on the surface of Fe@NCNTs. The gray balls represent C atoms, yellow for Fe, blue for N, red for O and white for H.

It is generally agreed that three elementary steps are involved for HER in acidic media.^{31,32} The first step is that a proton combines an electron to form adsorbed H atom, also known as the Volmer reaction (1). The adsorbed H atom has two possible routes to form the H_2 molecule and sequentially desorb, i.e. to react with a hydrated

proton from the electrolyte meanwhile receiving an electron from the CNTs surface, or to combine directly with another adsorbed H atom. The former reaction is called Heyrovsky mechanism (2) and the latter is known as the Tafel mechanism (3).



where the * denotes an active site on catalyst.

DFT calculations were also used to derive the reaction mechanism. The free energy profiles along intrinsic reaction coordinate (IRC) are shown in Figure 3b and 3c. The activation barrier of Fe@CNTs for Heyrovsky reaction is 1.02 eV, which is much lower than that of Tafel reaction (2.44 eV) as shown in Figure 3b. It indicates that the predominant route of HER in this catalytic system is via the Volmer-Heyrovsky mechanism, consistent with the analysis suggested by the experimentally measured Tafel slopes as indicated above. Moreover, from the free energy profiles of Heyrovsky route for pristine CNTs, Fe@CNTs and Fe@NCNTs (Figure 3c), the HER can hardly happen on pristine CNTs unless at a very high overpotential, due to the thermodynamically unflavored formation of H* intermediate. On the contrary, the HER can easily take place on Fe@CNTs and Fe@NCNTs by stabilizing the H* species.

In summary, 3d non-precious TM catalysts encapsulated in N-doped CNTs have been prepared through a simple CVD method, and the concentration of nitrogen could be modulated during the preparation of catalysts. These catalysts exhibited remarkable catalytic performance towards HER in acidic electrolyte. The optimized FeCo@NCNTs-NH catalyst showed an onset overpotential of only ~70 mV vs. RHE, which is amongst the smallest overpotentials of non-precious-metal HER catalysts in acidic electrolyte reported so far. Furthermore, these catalysts also showed a long-term durability during the 10000 cycles of accelerated degradation measurements. DFT calculations indicate that the adsorption free energy of H atom on CNTs can be decreased by the enclosed metal cluster and N-dopants, implying that

the introduction of metal and nitrogen in these catalysts can synergistically enhance the HER activity in accordance with the experimental results. Further calculations of free energy profiles along with intrinsic reaction coordinate indicate that the HER would likely occur through a Volmer-Heyrovsky mechanism in this system. These findings provide a new route in the design of efficient and durable non-precious-metal electrocatalysts for HER.

Acknowledgements

We gratefully acknowledge the financial support from the National Natural Science Foundation of China (No. 21303191), the strategic Priority Research Program of the Chinese Academy of Sciences (No. XDA09030100), and the Ministry of Science and Technology of China (No. 2012CB215500).

References

1. M. S. Dresselhaus and I. L. Thomas, *Nature*, 2001, **414**, 332-337.
2. J. A. Turner, *Science*, 2004, **305**, 972-974.
3. S. Schuldiner, *J. Electrochem. Soc.*, 1959, **106**, 891-895.
4. W. C. Sheng, H. A. Gasteiger and Y. Shao-Horn, *J. Electrochem. Soc.*, 2010, **157**, B1529-B1536.
5. I. A. Raj and K. I. Vasu, *J. Appl. Electrochem.*, 1990, **20**, 32-38.
6. A. Doner, I. Karci and G. Kardas, *Int. J. Hydrogen Energy*, 2012, **37**, 9470-9476.
7. A. Doner, R. Solmaz and G. Kardas, *Int. J. Hydrogen Energy*, 2011, **36**, 7391-7397.
8. V. V. Kuznetsov, A. A. Kalinkina, T. V. Pshenichkina and V. V. Balabaev, *Russ. J. Electrochem.*, 2008, **44**, 1350-1358.
9. M. Torabi and S. K. Sadrezaad, *Current Applied Physics*, 2010, **10**, 72-76.
10. R. Solmaz and G. Kardas, *Electrochim. Acta*, 2009, **54**, 3726-3734.
11. S. Kotrel and S. Braunigner, *Industrial Electrocatalysis*, Wiley-VCH Verlag GmbH&Co. KGaA, 2008.
12. B. Hinnemann, P. G. Moses, J. Bonde, K. P. Jorgensen, J. H. Nielsen, S. Horch, I. Chorkendorff and J. K. Nørskov, *J. Am. Chem. Soc.*, 2005, **127**, 5308-5309.
13. T. F. Jaramillo, K. P. Jorgensen, J. Bonde, J. H. Nielsen, S. Horch and I. Chorkendorff, *Science*, 2007, **317**, 100-102.
14. D. S. Kong, H. T. Wang, J. J. Cha, M. Pasta, K. J. Koski, J. Yao and Y. Cui, *Nano Lett.*, 2013, **13**, 1341-1347.
15. Y. G. Li, H. L. Wang, L. M. Xie, Y. Y. Liang, G. S. Hong and H. J. Dai, *J. Am. Chem. Soc.*, 2011, **133**, 7296-7299.
16. H. T. Wang, Z. Y. Lu, S. C. Xu, D. S. Kong, J. J. Cha, G. Y. Zheng, P. C. Hsu, K. Yan, D. Bradshaw, F. B. Prinz and Y. Cui, *Proc. Natl. Acad. Sci.*, 2013, **110**, 19701-19706.

17. J. F. Xie, H. Zhang, S. Li, R. X. Wang, X. Sun, M. Zhou, J. F. Zhou, X. W. Lou and Y. Xie, *Adv. Mater.*, 2013, **25**, 5807-5813.
18. J. F. Xie, J. J. Zhang, S. Li, F. Grote, X. D. Zhang, H. Zhang, R. X. Wang, Y. Lei, B. Pan and Y. Xie, *J. Am. Chem. Soc.*, 2013, **135**, 17881-17888.
19. A. B. Laursen, S. Kegnaes, S. Dahl and I. Chorkendorff, *Energy Environ. Sci.*, 2012, **5**, 5577-5591.
20. H. T. Wang, D. S. Kong, P. Johanes, J. J. Cha, G. Y. Zheng, K. Yan, N. A. Liu and Y. Cui, *Nano Lett.*, 2013, **13**, 3426-3433.
21. W. F. Chen, C. H. Wang, K. Sasaki, N. Marinkovic, W. Xu, J. T. Muckerman, Y. Zhu and R. R. Adzic, *Energy Environ. Sci.*, 2013, **6**, 943-951.
22. H. Vrubel and X. L. Hu, *Angew. Chem. Int. Ed.*, 2012, **51**, 12703-12706.
23. H. I. Karunadasa, E. Montalvo, Y. J. Sun, M. Majda, J. R. Long and C. J. Chang, *Science*, 2012, **335**, 698-702.
24. W. F. Chen, K. Sasaki, C. Ma, A. I. Frenkel, N. Marinkovic, J. T. Muckerman, Y. M. Zhu and R. R. Adzic, *Angew. Chem. Int. Ed.*, 2012, **51**, 6131-6135.
25. B. F. Cao, G. M. Veith, J. C. Neufeind, R. R. Adzic and P. G. Khalifah, *J. Am. Chem. Soc.*, 2013, **135**, 19186-19192.
26. D. H. Deng, L. Yu, X. Q. Chen, G. X. Wang, L. Jin, X. L. Pan, J. Deng, G. Q. Sun and X. H. Bao, *Angew. Chem. Int. Ed.*, 2013, **52**, 371-375.
27. J. Deng, L. Yu, D. H. Deng, X. Q. Chen, F. Yang and X. H. Bao, *J. Mater. Chem. A*, 2013, **1**, 14868-14873.
28. G. Wu, K. L. More, C. M. Johnston and P. Zelenay, *Science*, 2011, **332**, 443-447.
29. E. Proietti, F. Jaouen, M. Lefevre, N. Larouche, J. Tian, J. Herranz and J. P. Dodelet, *Nat. Commun.*, 2011, **2**, 416-424.
30. G. Liu, X. G. Li, P. Ganesan and B. N. Popov, *Appl. Catal. B-environ*, 2009, **93**, 156-165.
31. N. Pentland, J. O. M. Bockris and E. Sheldon, *J. Electrochem. Soc.*, 1957, **104**, 182-194.
32. B. E. Conway and B. V. Tilak, *Electrochim. Acta*, 2002, **47**, 3571-3594.
33. Z. B. Chen, D. Cummins, B. N. Reinecke, E. Clark, M. K. Sunkara and T. F. Jaramillo, *Nano Lett.*, 2011, **11**, 4168-4175.
34. J. Kibsgaard, Z. B. Chen, B. N. Reinecke and T. F. Jaramillo, *Nature Mater.*, 2012, **11**, 963-969.
35. M. A. Lukowski, A. S. Daniel, F. Meng, A. Forticaux, L. S. Li and S. Jin, *J. Am. Chem. Soc.*, 2013, **135**, 10274-10277.
36. D. Merki and X. L. Hu, *Energy Environ. Sci.*, 2011, **4**, 3878-3888.
37. D. Merki, H. Vrubel, L. Rovelli, S. Fierro and X. L. Hu, *Chem. Sci.*, 2012, **3**, 2515-2525.
38. E. J. Popczun, J. R. McKone, C. G. Read, A. J. Biacchi, A. M. Wiltrout, N. S. Lewis and R. E. Schaak, *J. Am. Chem. Soc.*, 2013, **135**, 9267-9270.
39. D. Voiry, H. Yamaguchi, J. W. Li, R. Silva, D. C. B. Alves, T. Fujita, M. W. Chen, T. Asefa, V. B. Shenoy, G. Eda and M. Chhowalla, *Nature Mater.*, 2013, **12**, 850-855.
40. Y. F. Xu, M. R. Gao, Y. R. Zheng, J. Jiang and S. H. Yu, *Angew. Chem. Int. Ed.*, 2013, **52**, 8546-8550.
41. J. Q. Zhuo, T. Y. Wang, G. Zhang, L. Liu, L. B. Gan and M. X. Li, *Angew. Chem. Int. Ed.*, 2013, **52**, 10867-10870.
42. J. K. Nørskov, T. Bligaard, A. Logadottir, J. R. Kitchin, J. G. Chen, S. Pandelov and U. Stimming, *J. Electrochem. Soc.*, 2005, **152**, J23-J26.